Atomic-scale structure of self-assembled In(Ga)As quantum rings in GaAs

P. Offermans, P. M. Koenraad, and J. H. Wolter
Department of Semiconductor Physics, Eindhoven University of Technology, P.O. Box 513, NL-5600 MB Eindhoven, The Netherlands

D. Granados and J. M. García
Instituto de Microelectrónica de Madrid, Isaac Newton, 8 — Parque Tecnológico de Madrid, 28760 Tres Cantos, Madrid, España

V. M. Fomin,[a] V. N. Gladilin,[b] and J. T. Devreese[c]
Theoretische Fysica van de Vaste Stoffen, Department Fysica, Universiteit Antwerpen, Universiteitsplein 1, B-2610 Antwerpen, België

(Received 24 February 2005; accepted 2 August 2005; published online 19 September 2005)

We present an atomic-scale analysis of the indium distribution of self-assembled In(Ga)As quantum rings (QRs) which are formed from InAs quantum dots by capping with a thin layer of GaAs and subsequent annealing. We find that the size and shape of QRs as observed by cross-sectional scanning tunneling microscopy (X-STM) deviate substantially from the ring-shaped islands as observed by atomic force microscopy on the surface of uncapped QR structures. We show unambiguously that X-STM images the remaining quantum dot material whereas the AFM images the erupted quantum dot material. The remaining dot material shows an asymmetric indium-rich crater-like shape with a depression rather than an opening at the center and is responsible for the observed electronic properties of QR structures. These quantum craters have an indium concentration of about 55% and a diameter of about 20 nm which is consistent with the observed electronic radius of QR structures. © *2005 American Institute of Physics*.
[DOI: 10.1063/1.2058212]

Quantum rings (QRs) are a special class of nanostructures that have attracted a lot of attention due to the occurrence of the Aharonov–Bohm effect, which is specific to the doubly-connected topology of a ring.[1–7] Particularly interesting are the magnetic properties of such quantum systems, which are related to the possibility of inducing persistent currents. In recent years the fabrication and investigation of self-assembled InAs QRs have been rapidly progressing and led to a large number of theoretical and experimental studies.[4,6,8–13]

In(Ga)As QRs are formed by capping self-assembled quantum dots (QDs) grown by Stranski–Krastanov (SK)-mode with a layer thinner than the dot height and subsequent annealing.[8] During this process, anisotropic redistribution of the QD material takes place, resulting in elongated ring-shaped islands on the surface, with crater-like holes in their centers as was shown with atomic force microscopy (AFM) measurements.[8] The dot to ring transition has been attributed to a dewetting process which expels indium from the QD,[14] and a simultaneous strongly temperature dependent Ga-In alloying process.[12]

Capacitance and far-infrared spectroscopy on buried QR structures have shown evidence of the first Aharonov–Bohm oscillation.[9] Although no direct measurements were available, an electronic radius of about 14 nm was deduced, what led to the conclusion that the QR shape as determined from AFM topography is preserved when buried.[9] Until recently,[15] however, no structural measurements of buried QRs have been available. Furthermore, measurements of the vertical Stark effect of excitons confined to individual QRs[11] have shown rather large dipole moments with opposite sign as compared to QDs.[16] Theoretical calculations have indicated that both the observed electronic radius and dipole moment of the QRs are inconsistent with the geometry as determined by AFM.[6] In order to unambiguously resolve this discrepancy we have analyzed the shape, size, and composition of buried QRs at the atomic scale by cross-sectional scanning-tunneling microscopy (X-STM).

Twenty layers of QRs separated by 18 nm were grown by solid source molecular-beam epitaxy (MBE) on a Si-doped n-type GaAs (001) substrate. The QRs are formed by the partial capping of InAs QDs grown at 540 °C with 2 nm of GaAs and subsequent annealing at 500 °C under As_2 flux.[12] On top of the structure a layer of QRs was grown for AFM measurements. The X-STM measurements are performed in an ultra-high-vacuum chamber on the orthogonal (110) and $(1\bar{1}0)$ cross-sectional surfaces. In X-STM the QRs are cleaved at a random position with respect to the center of the QR. Therefore, more than 100 QRs were imaged and the largest ones were selected for analysis. It can be then assumed that these QRs are cleaved near their middle. Photoluminescence measurements show identical results as observed for similar QR structures.[12,15]

Figure 1 shows an AFM image of the surface layer of the structure. The ring-shaped islands (density 10^{10} cm^{-2}) are elongated along the $[1\bar{1}0]$ direction, with an outer size of about 100 by 70 nm and an average height of about 1 nm. The holes in the center of the islands are asymmetric as well

[a] Also at: TU Eindhoven, P. O. Box 513, 5600 MB Eindhoven, The Netherlands; permanent address: Laboratory of Physics of Multilayer Structures, Department of Theoretical Physics, State University of Moldova, A. Mateevici 60, MD-2009 Chişinău, Moldova.
[b] Permanent address: Laboratory of Physics of Multilayer Structures, Department of Theoretical Physics, State University of Moldova, A. Mateevici 60, MD-2009 Chişinău, Moldova.
[c] Also at: TU Eindhoven, P. O. Box 513, 5600 MB Eindhoven, The Netherlands.

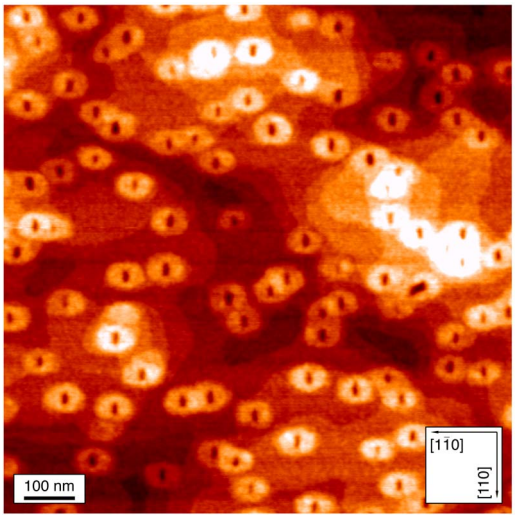

FIG. 1. (Color online) 1×1 μm^2 atomic force microscopy image showing the anisotropic distribution of InAs/GaAs dot material after 2 nm GaAs capping and 1 min annealing at growth temperature under As_2 flux. The height scale is 0 (dark) to 2.5 nm (bright). The height of the ring-shaped islands is about 1 nm. Atomic steps can be seen in the image.

and have a size of 30 by 20 nm and a depth of about 0.5–1.5 nm.

Figure 2 shows a large scale X-STM image of three of the QR layers. The rows in the image are the top rows of the cleaved (110) surface,[17] which are separated by one bilayer (BL), i.e., 0.565 nm, in the [001] direction. The bright spots correspond to In atoms in the top layer of the cleaved surface. In the image the cross-sections of two flat indium-rich nanostructures can be seen. Although these structures differ considerably from the ring-shaped islands as observed by AFM, see Fig. 1, we will discuss how they are related to each other.

In Fig. 3 we present averaged height profiles taken across the middle QR layer in the growth direction between the points A and B. The profiles are averaged over a distance of 10 nm in the [1$\bar{1}$0] direction and clearly indicate two peaks in the indium concentration. The highest peak can be attributed to the wetting layer on which the QDs are formed during growth. The separation between the peaks of 3–4 BLs corresponds to the height of the partial GaAs capping layer. This indicates that the formation of the second peak in the indium concentration occurs during the growth interruption after the partial capping of the QDs. We attribute the presence of the second indium layer to the accumulation of segregated indium from the wetting layer at the surface of the

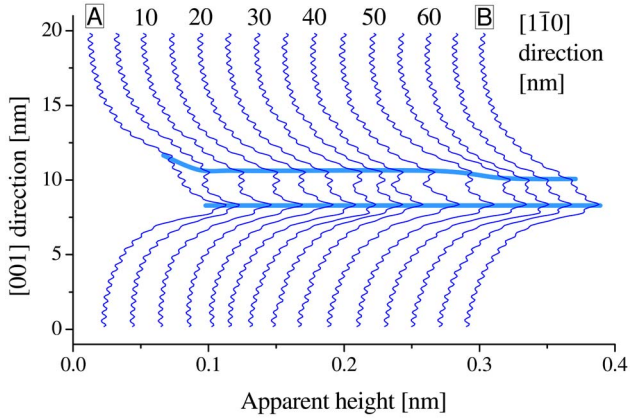

FIG. 3. (Color online) Averaged apparent height profiles taken in the growth ([001]) direction across the InAs layer between points A and B of Fig. 2. The height profiles are averaged over a distance of 10 nm and show two peaks in the indium concentration.

partial capping layer and to surface migration of indium atoms that have been expelled from the quantum dots during QR formation.[18–21]

We find that the second indium layer is not only present nearby the nanostructures, but actually extends laterally over the entire cleaved surface. However, by closer inspection of Fig. 2 or from the shaded lines in Fig. 3, it can be seen that over the distance between points A and B, the separation between the wetting layer and the second indium layer increases with about two bilayers towards the nanostructure. This change in separation is in agreement with the height and diameter of the uncapped QRs as measured by AFM. Thus at least to some extent the shape of the ring-shaped islands as observed by AFM is preserved after capping.

Enlarged views of the nanostructures can be seen in Fig. 4 where we show filled states topography images of the orthogonal (1$\bar{1}$0) and (110) cleavage planes, which correspond with the short and long axis of the ring-shaped islands observed by AFM, respectively.

The nanostructures have a crater-like shape which can be attributed to the remainder of the quantum dots after the QR formation process. It can be clearly seen that these quantum craters do not have an opening at the center. Furthermore, in the [110] direction, we generally find that the rim of the quantum crater appears brighter and higher (8 BLs) compared to the [1$\bar{1}$0] direction where the rim is less pronounced. We attribute this asymmetry to the preferential diffusion of the dot material in the [1$\bar{1}$0] direction[22] as can be seen from the elongation of the ring-shaped islands in Fig. 1.

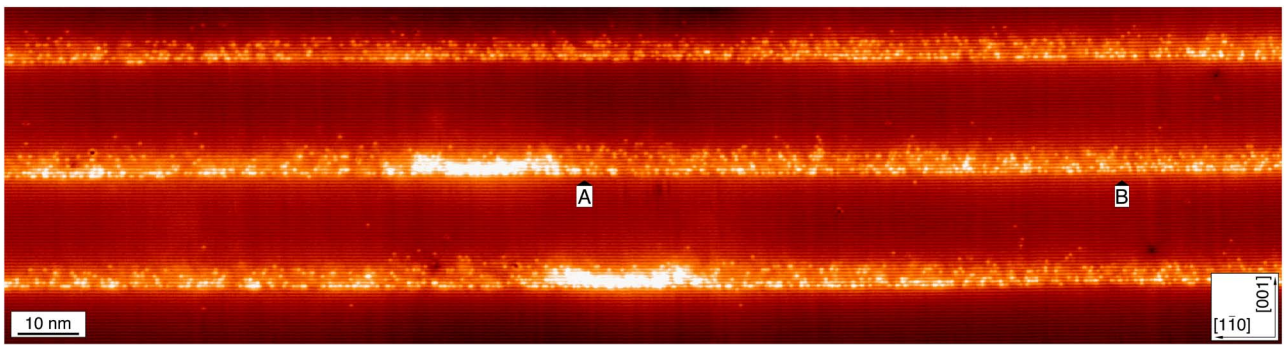

FIG. 2. (Color online) Empty states X-STM image showing two buried QRs, $V_{sample}=1.45$ V. The apparent height profiles shown in Fig. 3 are taken between the points A and B.

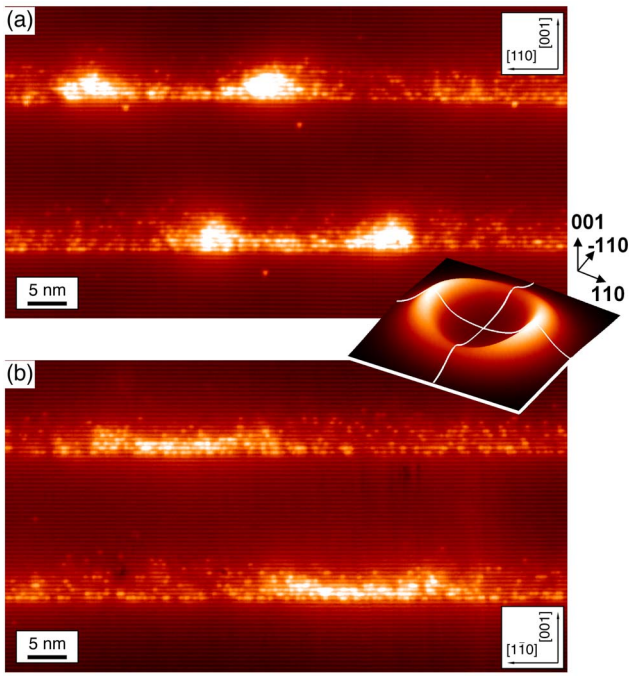

FIG. 4. (Color online) Filled states topography image of a cleaved QR in the $(1\bar{1}0)$ plane (a) and (110) plane (b), $V_{sample}=-3$ V. The height scale is 0 nm (dark) to 0.25 nm (bright). The inset shows the modeled QR.

The use of As_2 or high As_4 fluxes partially compensates this anisotropy.[12] The elongation of the ring-shaped islands at the surface implies that, compared to the [110] direction, in the $[1\bar{1}0]$ direction a larger fraction of the original InAs dot has been converted into the InGaAs rim observed by AFM. Therefore, it should be expected that the remaining dot material, i.e., the quantum crater, will present a less pronounced rim shape in the $[1\bar{1}0]$ direction.

By imaging at a high voltage ($V_{sample}=-3$ V), electronic contributions to the contrast in the image are minimized and only the true outward surface relaxation due to the lattice mismatch (7%) between the InAs and surrounding GaAs is imaged. We use the outward relaxation of the cleaved surface, to determine the indium composition of the quantum craters.[23,24] We model the quantum craters with a varying-thickness InGaAs layer embedded in an infinite GaAs medium. The bottom of the InGaAs layer is assumed to be perfectly flat and parallel to the *xy*-plane. The expression

$$h(\rho,\varphi) = h_0 + \frac{[h_M(1+\xi\cos 2\varphi) - h_0]\gamma_0^2}{R^2}\frac{R^2-(\rho-R)^2}{(\rho-R)^2+\gamma_0^2},$$

$$\rho \leqslant R,$$

$$h(\rho,\varphi) = h_\infty + \frac{[h_M(1+\xi\cos 2\varphi) - h_\infty]\gamma_\infty^2}{(\rho-R)^2+\gamma_\infty^2}, \quad \rho > R,$$

is used to describe the height of the InGaAs layer as a function of the radial co-ordinate ρ and the azimuthal angle φ, where h_0 corresponds to the thickness at the center of the crater, h_M to the rim height and h_∞ to the thickness of the InGaAs layer far away from the ring. The γ_0 and γ_∞ parameters define the inner and outer slopes of the rim, respectively. A three-dimensional finite element calculation based on elasticity theory has been used to calculate the relaxation of the cleaved surface of the modeled QR.

With $h_0=1.6$ nm, $h_M=3.6$ nm, $h_\infty=0.4$ nm, $\gamma_0=3$ nm, $\gamma_\infty=5$ nm, $\xi=0.2$ and $R=11.5$ nm and $R=10$ nm for the quantum craters in Figs. 4(a) and 4(b), respectively, we find that an indium concentration of $55\pm5\%$ results in a calculated surface relaxation that matches the measured relaxation of the cleaved surface.

In conclusion, we have performed an atomic scale analysis of the shape, size and composition of buried self-assembled QRs by cross-sectional scanning tunneling microscopy. We find that these structures show indium-rich asymmetric crater-like shapes which differ substantially from the ring-shaped islands on the surface of uncapped QR structures. Our conclusion that such quantum craters have a smaller size and a larger height than the ring-shaped islands, offers an explanation for the observed discrepancies between the measured and theoretical values for the electronic radius and dipole moment of the QRs.[6]

This work was partially supported by the GOA BOF UA 2000, IUAP, FWO-V projects G.0274.01N, G.0435.03, the WOG WO.035.04N (Belgium), the Spanish MCYT under NANOSELF project TIC2002-04096-C03-03 (Spain), the European Commission GROWTH Programme, NANOMAT project, contract No. G5RD-CT-2001-00545, and the European Commission SANDiE Network of Excellence, contract No. NMP4-CT-2004-500101.

[1] N. Byers and C. N. Yang, Phys. Rev. Lett. **7**, 46 (1961).
[2] M. Büttiker, Y. Imry, and R. Landauer, Phys. Lett. A **96**, 365 (1983).
[3] L. Wendler, V. M. Fomin, and A. A. Krokhin, Phys. Rev. B **50**, 4642 (1994).
[4] A. O. Govorov, S. E. Ulloa, K. Karrai, and R. J. Warburton, Phys. Rev. B **66**, 081309(R) (2002).
[5] M. Bayer, M. Korkusinski, P. Hawrylak, T. Gutbrod, M. Michel, and A. Forchel, Phys. Rev. Lett. **90**, 186801 (2003).
[6] J. A. Barker, R. J. Warburton, and E. P. O'Reilly, Phys. Rev. B **69**, 035327 (2004).
[7] S. Viefers, P. Koskinen, P. S. Deo, and M. Manninen, Physica E (Amsterdam) **21**, 1 (2004).
[8] J. M. García, G. Medeiros-Ribeiro, K. Schmidt, T. Ngo, J. L. Feng, A. Lorke, J. Kotthaus, and P. M. Petroff, Appl. Phys. Lett. **71**, 2014 (1997).
[9] A. Lorke, R. J. Luyken, A. O. Govorov, J. P. Kotthaus, J. M. García, and P. M. Petroff, Phys. Rev. Lett. **84**, 2223 (2000).
[10] R. J. Warburton, C. Schäflein, D. Haft, F. Bickel, A. Lorke, K. Karrai, J. M. García, W. Schoenfeld, and P. M. Petroff, Nature (London) **405**, 926 (2000).
[11] R. J. Warburton, C. Schulhauser, D. Haft, C. Schäflein, K. Karrai, J. M. García, W. Schoenfeld, and P. M. Petroff, Phys. Rev. B **65**, 113303 (2002).
[12] D. Granados and J. M. García, Appl. Phys. Lett. **82**, 2401 (2003).
[13] T. Raz, D. Ritter, and G. Bahir, Appl. Phys. Lett. **82**, 1706 (2003).
[14] R. Blossey and A. Lorke, Phys. Rev. E **65**, 021603 (2002).
[15] D. Granados, J. M. García, T. Ben, and S. I. Molina, Appl. Phys. Lett. **86**, 071918 (2005).
[16] P. W. Fry *et al.*, Phys. Rev. Lett. **84**, 733 (2000).
[17] R. M. Feenstra, J. A. Stroscio, J. Tersoff, and A. P. Fein, Phys. Rev. Lett. **58**, 1192 (1987).
[18] L. G. Wang, P. Kratzer, M. Scheffler, and Q. K. K. Liu, Appl. Phys. A: Mater. Sci. Process. **73**, 161 (2001).
[19] Z. R. Wasilewski, S. Fafard, and J. P. McCaffrey, J. Cryst. Growth **201/202**, 1131 (1999).
[20] E. Steimetz, T. Wehnert, H. Kirmse, F. Poser, J.-T. Zettler, W. Neumann, and W. Richter, J. Cryst. Growth **221**, 592 (2000).
[21] A. Lenz, H. Eisele, R. Timm, S. K. Becker, R. L. Sellin, U. W. Pohl, D. Bimberg, and M. Dähne, Appl. Phys. Lett. **85**, 3848 (2004).
[22] K. Shiraishi, Appl. Phys. Lett. **60**, 1363 (1992).
[23] P. Offermans, P. Koenraad, J. Wolter, K. Pierz, M. Roy, and P. Maksym, Physica E (Amsterdam) **26**, 236 (2005).
[24] D. M. Bruls, J. W. A. M. Vugs, P. M. Koenraad, H. W. M. Salemink, J. H. Wolter, M. Hopkinson, M. S. Skolnick, F. Long, and S. P. A. Gill, Appl. Phys. Lett. **81**, 1708 (2002).